

Valve controlled fluorescence detection system for remote sensing applications

T. D. James · M. G. Scullion · P. C. Ashok ·
A. Di Falco · K. Dholakia · T. F. Krauss

Received: 28 February 2011 / Accepted: 15 May 2011
© Springer-Verlag 2011

Abstract We demonstrate a microfluidics-based fluorescence detection device where the filters, source, detector, and electronically controlled valves are embedded into a Polydimethylsiloxane (PDMS)-based microfluidic chip. The device reported here has been specifically designed for chlorophyll a fluorescence sensing in autonomous systems, such as oceanic applications. In contrast to a monolithic approach, the modular approach made the fabrication of this device simpler and cheaper. For fluorescence detection, an InGaN/GaN LED is used as the excitation source to specifically excite chlorophyll a; a metal-dielectric Fabry–Perot filter was used to extinguish out-of-band excitation. A simple Si photodiode is used as detector and provided with a thermally evaporated CdS emission filter to block the excitation source. This filter combination provides an excellent solution to the difficult problem of combining high-rejection excitation and emission filters in an integrated thin-film format. Furthermore, the metal-dielectric filter provides a much broader angular response than a comparable multilayer Bragg mirror, which is a key advantage in the integrated format. We use a novel paraffin wax-based valve design affords low power single-use actuation, between 0.5 and 1 J per actuation and withstands 0.6 bar differential pressure, which provides better performance than its previously reported counterparts. The remote valve-controlled operation of the fluorescence detection system is demonstrated, illustrating the measurement of a chlorophyll a solution, with a detection limit

of 340 μM and subsequent valve-controlled flushing of the measurement reservoir.

Keywords Fluorescence detection · Microvalve · Hybrid design · Microfluidics

1 Introduction

Fluorescence imaging and detection is an ever-expanding biological analysis technique based on the rapid development of both fluorescent probes and novel instrumentation. Fluorescence spectroscopy instruments, initially desktop-type laboratory tools, have now been significantly reduced in size and cost by leveraging microelectronics-based sources, detectors, and optical components. As a result, current commercial devices used for applications in the field have been reduced to hand-held sized tools that are typically attached to a data-logging unit and that are using a fluid flow-through design approach (Turner Designs Inc.; CTG Inc.). Truly miniaturized devices operating on a cm or mm scale that can subsequently be integrated to enable multimodal analysis and operate with low power consumption are only in their infancy (Chabinyc et al. 2001; Chediak et al. 2004; Kamei et al. 2003; Thrush et al. 2005; Yao et al. 2005). Some of the limitations of the published work on micro-fluorescence detection systems include the use of high-power laser sources or high-power detectors such as avalanche photodiodes or photomultiplier tubes, which make the system unsuitable for remote sensing applications due to large operating power demands (Chabinyc et al. 2001; Kamei et al. 2003; Yao et al. 2005). Fully integrated fluorescence excitation/detection devices have been demonstrated, however, the excitation wavelength is too stimulate most fluorophores severely limiting

T. D. James (✉) · M. G. Scullion · P. C. Ashok · A. Di Falco ·
K. Dholakia · T. F. Krauss
SUPA, School of Physics and Astronomy, University
of St Andrews, North Haugh, St Andrews, Fife KY16 9SS,
Scotland, UK
e-mail: tdj21@st-andrews.ac.uk

the application of the device (O'Sullivan et al. 2010). Another limitation is that many device architectures are only able to capture a small percentage of the fluorescence signal, which results in relatively low performance (Chediak et al. 2004; Thrush et al. 2005). Our study is focused on both the development of a low power, highly efficient micro-fluorescence system and its integration with a low power valve controlled microfluidic system and we show that high performance can be achieved on a small footprint with low operating power requirements.

The full miniaturisation of a fluorescence detection system requires more than just the shrinking of the excitation source and the fluorescence detector, i.e., it also involves the miniaturisation of the analyte control and processing mechanisms. The targeted fluorophore in this study is chlorophyll a, which is a vitally important indicator for the study of climate change, ocean toxicity, and food security in the marine environment. The development of a low powered valve controlled system enables the future advancement of lab-on-chip based analyte processing of chlorophyll a, which is therefore of great importance. Typically, chlorophyll a from marine environments is found in phytoplankton, i.e., microscopic plant organisms, and is relatively difficult to detect due to its low concentration. On a microfluidic chip, however, one could realise the chemical extraction of chlorophyll a from the phytoplankton, thus greatly improving the sensitivity and accuracy of the measurement (Maxwell and Johnson 2000). This could be achieved by mixing the analyte with solvents from an on-chip reservoir, extracting the chlorophyll a and then delivering the solution to the fluorescence measurement chamber. The demonstration of microfluidic circuitry integrated with a fluorimeter is therefore of great interest and provides the motivation for this article.

Our system consists of PDMS-based microfluidic channels that feed the analyte into a fluorimeter driven by an energy-efficient GaN LED source with a solid-state silicon photodiode and thin film metal/dielectric and absorption filters for detection, with low power, micro-heater driven, wax-based valves for analyte control.

2 Device design

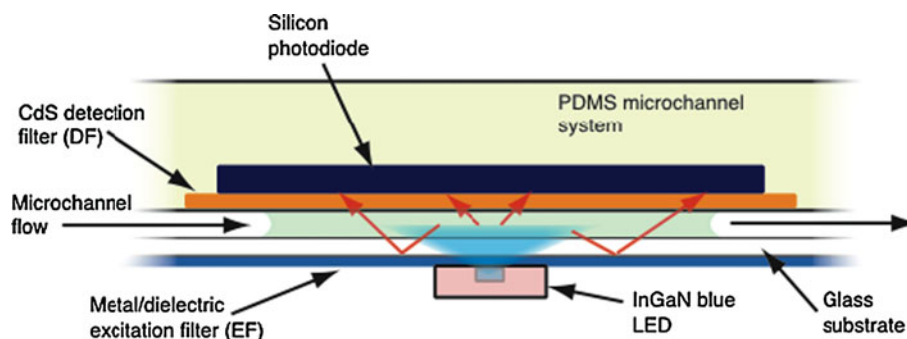
2.1 Fluorescent detection

A cross-sectional diagram of the fluorescence detection system is presented in Fig. 1, where the analyte flows through a PDMS microchannel between the excitation source and the detector. The excitation section of the device consists of a very compact ($0.8 \times 1.1 \times 1.6 \text{ mm}^3$), low-cost InGaN/GaN-based LED with a peak emission wavelength of 430 nm (Kingbright KP-1608MBC). The target analyte, chlorophyll a, has an emission peak at a wavelength of 662 nm that is collected by a Si detector ($5.1 \times 5.1 \text{ mm}^2$ photodiode, Silonex SLSD-71N200), which is located on the opposite side of the microchannel to the source. The detector is embedded into the PDMS and is placed as closely as possible to the channel to maximise the captured fluorescence signal.

To achieve the highest possible detection sensitivity, the detector should be completely shielded from the excitation source signal, yet be able to detect light unimpeded at the fluorescence wavelength. This is accomplished by using two filters, one at the excitation source and the other at the detector, working together to blind the detector to the excitation source while still maintaining sensitivity to the fluorescence signal. The excitation source filter (EF) passes the low wavelength signal of the excitation source (430 nm), while attenuating any signal the source produces at the fluorescence signal wavelengths (662 nm). The detector filter (DF) is designed to block the excitation source while passing the fluorescence source. When working in conjunction with the EF, the detector is only sensitive to the fluorescence signal. Incorporating these filters into our integrated fluorescence detection device is a key issue that requires novel solutions, as standard off-the-shelf filters are too bulky with thicknesses in the order of mm's, which move the detector too far away from the fluorescence source to detect any significant signal.

For the EF, we have chosen a metal/dielectric Fabry–Perot filter design for its many specific advantages over other thin film filter designs for the given application. The

Fig. 1 Cross-section of a single channel microfluidic measurement setup for fluorescence sensitivity measurements, illustrating the excitation signal from the LED, resulting in emission (arrows) from the analyte in the microchannel reaching the silicon detector



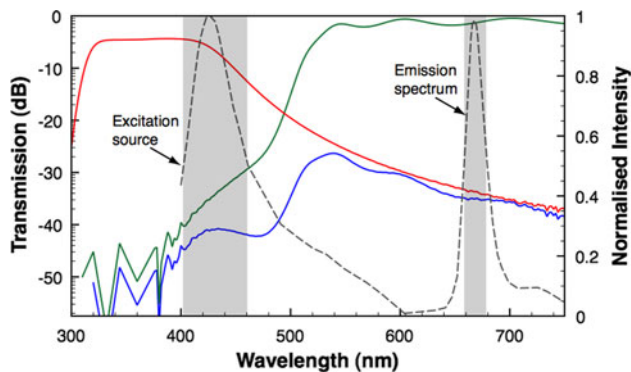


Fig. 2 Experimental transmission curves of excitation (EF) and detection filters (DF) used in the fluorescence detection device along with the combined transmission of both filters. The *gray* sections illustrate the FWHM of the excitation LED output and Chlorophyll a fluorescence emission spectra, overlaid in *dashed gray* curves in normalized units

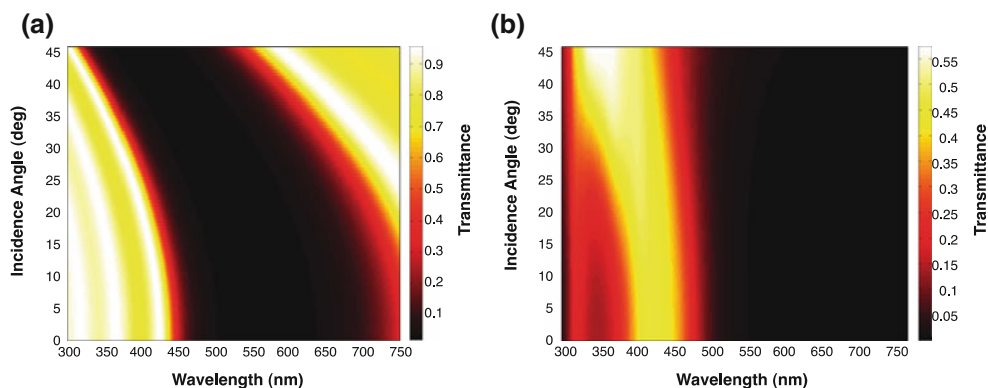
particular metal/dielectric EF used was fabricated by e-beam evaporation and made up of five layers consisting of Ag/MgF₂/Ag/MgF₂/Ag, with thicknesses of 20/110/40/110/20 nm, respectively, whose transmittance spectrum is shown in Fig. 2. The metal/dielectric design is more tolerant to fabrication errors of layer thickness compared to an all-dielectric-based thin film filter, and has the properties of an absorption filter at long wavelengths (Macleod 2001). The metal/dielectric design also reduces the number of layers and thickness of material required as compared to the all-dielectric short pass filters. There is a trade-off, however, as the peak transmission for a metal/dielectric filter is typically less than half that of an all-dielectric filter. Nonetheless, the reduction of signal from the excitation source in the fluorescence spectral region is of far more importance than of the reduction in excitation signal, due to the weakness of the fluorescence signal at low sample concentrations and the excitation source only needing to illuminate a minute volume of analyte in the microchannel.

In addition, metal/dielectric filters are more robust to variations in the angle of incidence of light than all-

dielectric filters, which is essential for accommodating the non-collimated nature of the LED excitation source. In the case of the design presented in Fig. 1, the light incident on the EF from the excitation source ranges from 0° to 45°. The corresponding angular dependence of the metal/dielectric EF filter transmittance is presented in Fig. 3, along with that of a comparable all-dielectric filter. In the calculations, the all-dielectric filter is made up of four pairs of low and high refractive index material, 1.3 and 2.5, respectively, resulting in a total thickness of 759 nm, over twice the thickness of the metal/dielectric EF used in this study. At the excitation wavelength of 430 nm, the transmission of the all-dielectric filter varies between 87.5 and 0.37% for a change of angle from 0 to 30°, whereas the metal/dielectric filter only varies between 40 and 44.6%, highlighting the improvement.

A thin film of CdS works perfectly as DF due to the direct band-gap of the semiconductor creating a sharp absorption edge at 510 nm, as shown in Fig. 2. CdS thin films are typically deposited via chemical bath deposition (CBD) or sputtering techniques (Chediak et al. 2004; Durose et al. 1999). However, CdS thin films created via CBD/sputtering tend to show large amounts of surface roughness that causes optical loss, and it is also difficult to fabricate thin films of greater than 300 nm thicknesses in the case of CBD (Nemec et al. 2002). A CdS deposition technique less commonly used is thermal evaporation, where thin films of CdS in excess of 1 μm can be easily deposited without any significant surface roughness (Duke et al. 1996). The increased thickness and reduced surface roughness of thin films fabricated by thermal evaporation enhance the extinction and transmission characteristics, respectively, of the resulting filter. We used 750 nm thickness and the film was thermally evaporated on a glass substrate at room temperature under a vacuum of approximately 6×10^{-6} Torr. The optical characteristics of the filter are presented in Fig. 2, showing 80% transmission in the pass-band region ($\lambda > 510$ nm), which is nearly twice the typical value achieved with CdS thin films deposited by CBD or sputtering (Chediak et al. 2004).

Fig. 3 Simulations of the transmittance of an 8 layer all-dielectric short-pass filter (a), and the metal-dielectric Fabry–Perot filter used in this study (b)



The transmission functions of both the DF and EF (acquired for normal incidence with a Perkin-Elmer Lambda spectrometer) and the combined response are shown in Fig. 2. The grayed areas shown in Fig. 2 highlight the spectral ranges full-width-half-maximum of the LED excitation source, taken from the manufacturers data sheet, and the fluorescence emission peak of Chlorophyll a (Papageorgiou 2004), along with their respective spectra. The combined transmission spectrum of the filters shows that the detector will observe less than 0.008% of the peak output of the LED at a wavelength of 430 nm, while even at the filter's weakest point (540 nm) the transmittance is only 0.022%. The only loss of fluorescence signal of the DF is due to reflections at the interface between glass and CdS caused by the refractive index difference of the materials (between 10 and 15% depending on the wavelength), as shown in the CdS curve of Fig. 2. This interface reflection loss could be reduced with the simple application of dielectric anti-reflection coatings.

The hybrid integrated design of the fluorescence detection system with the microfluidic analyte delivery technique allows a great improvement in the collection efficiency of fluorescence signal, as compared to other designs where the microfluidics sits on top of the fluorescence detection device (Chabinyk et al. 2001; Chediak et al. 2004; Kamei et al. 2003; Thrush et al. 2005). The EF is highly reflective in the spectral region where the chlorophyll a fluorescence occurs, so acts as a mirror for the fluorescence signal that is emitted directly away from the detector. This effectively doubles the amount of collectable signal available compared to if the source and detector were on the same plane with no reflective element (Chabinyk et al. 2001; Chediak et al. 2004; Kamei et al. 2003; Thrush et al. 2005).

2.2 Integrated microfluidic system

The miniaturisation and integration of analyte control tools is critical to the development of an autonomous fluorescence detection system. To reduce the physical size and energy consumption of the analyte control system, microfluidic channels are used for sample delivery to the detection region. The hybrid nature of the fluorescence detection system requires the detector/DF to be embedded into the PDMS-based microfluidic system, which consists of both microchannels and microvalves. The channels, into which we integrate both the valves and fluorescence detection system, are created in Polydimethylsiloxane (PDMS) using standard soft lithography techniques.

An SU-8 photoresist (Microchem) blend of one part 2000.5 to ten parts 2050 is spun to a thickness of 40 μm on a cleaned piece of silicon, before baking at 65°C for 5 min and 95°C for 15 min on a hotplate. The soft baked sample

is then exposed to UV through a photomask of the microchannel design in a mask aligner. Following a post-exposure bake at 65°C for 1 min and 95°C for 15 min, the sample is developed in EC solvent, rinsed in de-ionized (DI) water and left overnight in a 175°C oven for hard baking. This creates a positive mould for the microchannel design.

The detector and DF are bonded together using a drop of PDMS as an adhesive and then placed on top of a silanised piece of PDMS membrane (cut to similar area as the DF) in a petri dish. PDMS base and curing agent (Sylgard 184) are mixed in a ratio of 10:1, degassed and poured over the finished mould, before being placed in a 60°C oven for over 4 h. The silanized layer of PDMS is used as a sacrificial membrane in the embedding process, as it stops air bubbles from forming underneath the detector/DF, creating a uniform air gap once removed to facilitate the efficient bonding of the thick and microchannel PDMS layers. The cured PDMS containing the detector and DF is then peeled from the mould.

We then integrate membrane-based microvalves into these channels using multiple PDMS layers. This design relies on deformation of the fluid channel via pressure from a wax chamber, and was chosen for its relative ease of fabrication, small size, ability to be actuated electrically, and simplicity compared to pneumatic valves (Unger et al. 2000). The fact that they can only be actuated once is not an issue for the remote application we envisage, as each microchannel would provide the analyte for a single measurement. The valves are fabricated by spinning PDMS at 500 rpm on the as described microchannel mould and curing on a 120°C hotplate for 5 min. Once the thick PDMS layer containing the detector/DF is peeled from the petri dish, it is cut to size, and wax inlet holes punched, which then forms the top layer of the microvalve structure, as shown in Fig. 4. The thick layer encasing the detector/DF is then aligned and bonded to the first membrane layer of PDMS containing the microfluidic channels using a coronal discharge gun, methanol, and baking in a 60°C oven. The bonded structure is then peeled from the mould and inlets punched through all layers to the channels to allow analyte injection. This is bonded to a glass slide in the same manner as before, forming the bottom lid of the channel.

To minimize both the size and power consumption of the valves, microheaters were chosen as actuators rather than bulkier structures such as peltier heaters used in other wax valves (Liu et al. 2004). Microheaters are integrated into this glass slide using photolithographic patterning in AZ 4562 resist, evaporation of 200 nm of aluminium in a thermal evaporator and lift-off of the redundant metal in acetone. Tacky microcrystalline wax is loaded into the relevant holes in the top layer, deforming the membrane

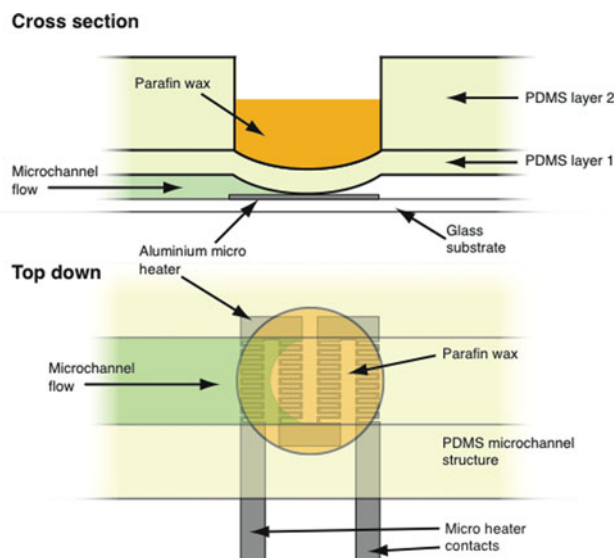


Fig. 4 Cross-section and top down diagram of microheater controlled wax-based microchannel valves

and hence channel region below it, as shown in Fig. 4. Actuation is achieved by passing a current through the microheaters. In the device fabricated here, six valves were incorporated into the design. These have a footprint as small as the wax chamber, in this case a hole of 2 mm diameter, allowing for tens of these on a centimeter scale chip. Reducing this size further would allow even greater densities of valves to be used. Tests showed the valves could be actuated in under 1 s using 0.5–1 J of energy, which compares favorably to other wax valves that require between 1 and 5 Joules to actuate (Liu et al. 2004; Pal et al. 2004) and is due to the smaller size of the wax chamber and heating element. The microcrystalline wax used here has a relatively high melting point of 68°C. Using a lower melting point wax or smaller amounts of wax (for example, halving the amount of wax would half the energy required to melt it) could reduce energy consumption further.

Pressure resistance was tested by connecting pressurized argon to a tube containing colored water, which in turn was connected to a fluid inlet port on the chip. Pressure on the fluid was controlled using a regulator on the argon supply. Using this setup, the valves were able to withstand a differential pressure of 0.6 bar. This is an improvement over a comparable wax-based membrane valve (Yang and Lin 2007), which withstood 0.35 bar, due to the higher density and adhesive properties of microcrystalline wax compared to paraffin. The valve presented here has the added advantage that it is fully integrated with microheaters. Plug-based wax microvalves, which consist of regions of wax within the microchannel, can withstand significantly higher pressures than membrane based valves, with pressure resistances of 2.7 bar (Liu et al. 2004) and even 17.2 bar having been achieved (Pal et al. 2004). Membrane

valves, however, have the advantage that the wax is kept separate from the channel contents, eliminating possible contamination. Pressure resistance could be improved by designing curved, rather than rectangular, channels (Unger et al. 2000).

3 Results and discussions

3.1 Fluorescence detection

In order to characterize the performance of the detection system, we measured the fluorescence of chlorophyll a, in a simplified geometry, shown in Fig. 1. The microchannel used for the measurements has the dimensions of 2 mm wide by 1 mm high, where the analyte was injected by syringe. For the intended autonomous applications, the analyte would be driven by fluidic pressure or capillary action into the microfluidic channel (Zimmermann et al. 2007), rather than being driven by a mechanical pump or syringe based device, allowing the low power microfluidics valves to control the flow of analyte. The microchannel dimensions were chosen to simulate a large deep measurement reservoir used to increase the relative sensitivity, and to simplify the fabrication procedure of the test device.

Notably, chlorophyll a has a relatively low fluorescence quantum efficiency, typically around 3% (Krause and Weis 1991), compared to the fluorophores commonly used in the literature, such as fluorescein, which has a quantum efficiency of approximately 95% (Brannon and Magde 1978). This feature of chlorophyll a makes it a challenging fluorophore to work with. The chlorophyll a used in this study was sourced from Sigma-Aldrich and is derived from spinach. It was diluted in ethanol to the required concentrations and kept in a freezer between measurements as per the manufacturers instructions. The samples were kept in dark brown bottles, and shielded from ambient laboratory light as much as possible to reduce photobleaching prior to measurement. However, it was unavoidable that the samples were exposed to small amounts of room light prior to the experiments, typically 30 s to 1 min.

The fluorescence measurements were performed as follows; the microchannel is first flushed with de-ionised (DI) water, a measurement is taken to determine the background signal of the setup, the chlorophyll a solution is then fed into the microchannel and measured. Finally, the microchannel is flushed again with DI water in order to perform a second background measurement. This provides two background measurements for each fluorescence sample in order to confirm the validity of the measurement.

Fluorescence measurements of chlorophyll a solutions with a range of concentrations are presented in Fig. 5. The

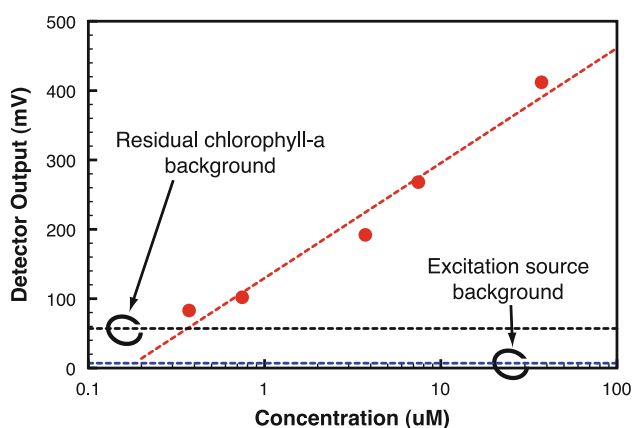


Fig. 5 Measurement of chlorophyll a fluorescence with single microchannel fluorescence detection device showing the measurement background due to the excitation source and residual chlorophyll a

background emanating from the excitation source is very low, approximately 7 mV, which is marginally larger than the thermal noise of the transimpedance amplifier used to extract the signal from the photodiode. The second background signal is due to residual chlorophyll a left in the microchannel after numerous measurements. This is due to chlorophyll a in the ethanol/chlorophyll a solution depositing on the walls of the microchannel, which cannot be washed away with water. Residual background fluorescence is only an issue for this test device, as for a valve controlled device a fresh channel would be used for each measurement. This means that the background signal observed for a valve controlled device would simply be due to the very small leakage of the excitation source signal to the detector, as shown by the 7 mV line in Fig. 5. However, the residual chlorophyll a background noise was consistent throughout the series of measurements with the single channel test device, and amounted to approximately 57 mV. The fluorescence detection results presented in Fig. 5 all displayed the same background signal, both before and after measurement.

The fluorescence detection displays the typical linear behavior between concentration and detector output signal

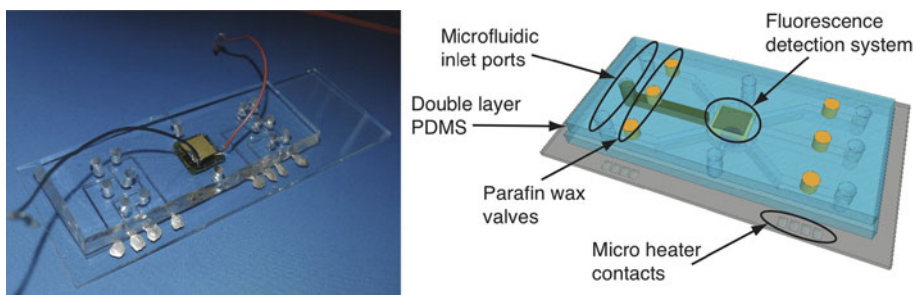
that one would expect, with the minimum detected solution concentration of 340 nM of chlorophyll a diluted in ethanol. This result compares very well with other LED-based fluorescence detection systems, where detection limits are in the order of 100's of nM (Chediak et al. 2004; Thrush et al. 2005; Yao et al. 2005). However, the results presented in the literature are achieved using fluorophores with high quantum efficiency, typically over 20 times that of chlorophyll a. Using such high-efficiency fluorophores would give our device a sensitivity of 10's of nM compared to the devices presented elsewhere.

3.2 Valve controlled fluorescence detection

Figure 6 presents a diagram and photograph of the fluorescence detection system integrated with the wax-based valve controlled fluorescence detection system. The integrated valve controlled fluorescence detection system consists of a common analyte chamber and six feeding channels, which are independently addressed by the six electronically operated wax valves, plus a reset channel for laboratory experiment control. The analyte chamber in the valve controlled microfluidic system is smaller in volume than that of the single channel used to demonstrate the sensitivity of the fluorescence detection system. This was done to simplify the fabrication process of the valve controlled microchannel device by using a single channel depth for the whole device. The aim of this study is to demonstrate a proof-of-principle device with a valve controlled fluorescence measurement, and not an absolute representation of the device's sensitivity.

The power consumption of the valve controlled microfluidic fluorescence detection system has been calculated per measurement, which involves the opening of a valve and operation of the source driver and detector amplifier electronics for one second. As previously mentioned, the valve consumes between 0.5 and 1 J, and the combined operation of source/detector electronics was 0.11 J per 1 s measurement, resulting in maximum single measurement power consumption of 1.11 J. This number could be further reduced by performing Fast Repetition Rate fluorescence measurements, whereby the source/detector electronics are

Fig. 6 Photograph and diagram of the integrated valve controlled microchannel device with integrated fluorescence detection system



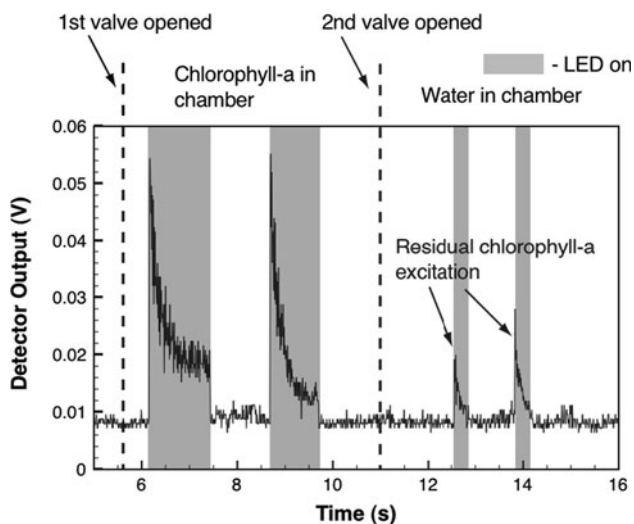


Fig. 7 Measured fluorescence signal during operation with chlorophyll a first, then after flushing with deionised water using valves to control the flow into the measurement reservoir

often powered for a tenth of a second or less (Suggett et al. 2003). The power consumption of the device presented in this study is comparable to commercially available devices based on a much simpler flow-through system (Turner Designs Inc.; CTG Inc.), which as previously stated has issues with measurement smear and reproducibility.

Operation of the valve-controlled device is presented in Fig. 7. The first valve is opened and the chlorophyll a/ethanol solution is drawn into the measurement reservoir, the fluorescence is measured with two distinct pulses from the excitation source. The typical exponential decay of chlorophyll a fluorescence is observed for each pulse, referred to as the Kautsky effect, and is related to the photochemical efficiency of the chlorophyll a molecule (Maxwell and Johnson 2000). After the measurement, a second valve is opened and the reservoir is flushed with DI water and measured again, where the residual chlorophyll a fluorescence is observed. This represents the typical operation of such a device in a remote sensing application. Valves would be automated or controlled remotely drawing in the analyte, then allowing the flushing of the measurement reservoir to provide a background measurement for reference, and to show the device is operating as expected.

The result presented in Fig. 7 shows a proof-of-principle for a wax-based valve controlled fluorescence detection system for remote sensing applications. There is considerable scope for improvement in the performance of the fully integrated device, for example by optimizing the microfluidic dimensions, and increasing the sensitivity of the integrated fluorescence detection system through higher powered sources and more sophisticated electronic signal processing and data collection techniques (e.g., implementing time integration). The demonstration of a valve

controlled microfluidic system enables the development of greater functionality with respect to analyte processing to further improve the fluorescence detection performance. Such functionality could include the controlled flushing of the measurement reservoir with a chlorophyll a cleaning solution, or provide the ability to extract chlorophyll a from within the microscopic oceanic plants via steeping/heating/sonication the sea water in solvents introduced from a on chip reservoir, which would greatly improve the fluorescence yield (Krause and Weis 1991). With such improvements, we hope to achieve single nM chlorophyll a sensitivities, which would meet the sensitivity requirements for measuring chlorophyll a in the marine environment of typically 0.1–11 nM (Cota et al. 2004; Kiefer et al. 1989).

4 Conclusions

We have presented a proof of principle demonstration of a fully integrated, valve controlled microfluidic fluorescence detection system. The fluorescence detection system exhibits a high degree of sensitivity to chlorophyll a, an important fluorophore in the fields of oceanic monitoring, climate change study, and food security. The fluorescence sensitivity of the device was measured at 340 nM for chlorophyll a in ethanol. This result matches the performance of other LED-based fluorescence detection systems, yet it has been achieved with a fluorophore with at least one order of magnitude lower fluorescence efficiency. The wax-based microheater controlled valves demonstrated very low power usage, between 0.5 and 1 J per actuation, making them very suitable for remote sensing applications, where simple low power electronic control is highly desirable. Several improvements can be made to further improve the performance of the device in order to achieve a similar sensitivity as the current commercial systems, which are orders of magnitude more bulky and quite power-hungry. The most obvious way to reduce the detection limit is to use a DF made up of a ternary semiconductor comprising of CdS/CdSe, where the band-gap or cut-off wavelength can be tuned to between 513 and 712 nm, which would further reduce the background signal observed by the silicon detector. Other ways to improve the fluorescence detection sensitivity include improving the microchannel design to maximize the fluorescence signal, development of channel cleaning techniques and increased sensitivity of the fluorescence detection system via higher power excitation sources, and improved detection signal processing. This study provides a working demonstration of a valve controlled microfluidic fluorescence detection device and creates further opportunities to add greater functionality to current remote sensing techniques.

Acknowledgments We gratefully acknowledge funding for the project through EPSRC EP/F020589/1, and Andrea Di Falco is supported by an EPSRC Career Acceleration Fellowship (EP/I004602/1). We also acknowledge the helpful discussions with Dr Bernie McConnell, Dr Ailsa Hall and Prof Mike Fedak from the Sea Mammal Research Unit in the School of Biology at the University of St Andrews.

References

- Brannon J, Magde D (1978) Absolute quantum yield determination by thermal blooming—fluorescein. *J Phys Chem Us* 82(6):705–709
- Chabinyk M, Chiu D, McDonald J, Stroock A, Christian J, Karger A, Whitesides G (2001) An integrated fluorescence detection system in poly(dimethylsiloxane) for microfluidic applications. *Anal Chem* 73(18):4491–4498. doi:10.1021/ac010423z
- Chediak J, Luo Z, Seo J, Cheung N, Lee L, Sands T (2004) Heterogeneous integration of CdS filters with GaN LEDs for fluorescence detection microsystems. *Sensor Actuat A Phys* 111(1):1–7. doi:10.1016/j.sna.2003.10.015
- Cota G, Wang H, Comiso J (2004) Transformation of global satellite chlorophyll retrievals with a regionally tuned algorithm. *Remote Sens Environ* 90(3):373–377. doi:10.1016/j.rse.2004.01.005
- CTG Inc. <http://www.chelsea.co.uk/Instruments%20AQUAtracka.htm>. Accessed 4 Sept 2010
- Duke S, Miles R, Pande P, Spoor S, Ghosh B, Datta P, Carter M, Hill R (1996) Characterisation of in situ thermally evaporated CdS/CdTe thin film solar cells with Ni-P back contacts. *J Cryst Growth* 159(1–4):916–919
- Durose K, Edwards P, Halliday D (1999) Materials aspects of CdTe/CdS solar cells. *J Cryst Growth* 197(3):733–742
- Kamei T, Paegel B, Scherer J, Skelley A, Street R, Mathies R (2003) Integrated hydrogenated amorphous Si photodiode detector for microfluidic bioanalytical devices. *Anal Chem* 75(20):5300–5305. doi:10.1021/ac0301550
- Kiefer D, Chamberlin W, Booth C (1989) Natural fluorescence of chlorophyll-a—relationship to photosynthesis and chlorophyll concentration in the western south-pacific gyre. *Limnol Oceanogr* 34(5):868–881
- Krause G, Weis E (1991) Chlorophyll fluorescence and photosynthesis—the basics. *Ann Rev Plant Phys* 42:313–349
- Liu RH, Bonanno J, Yang J, Lenigk R, Grodzinski P (2004) Single-use, thermally actuated paraffin valves for microfluidic applications. *Sensor Actuat A Phys* 98:328–336
- Macleod HA (2001) Thin-film optical filters, 3rd edn. Institute of Physics Publishing, London
- Maxwell K, Johnson G (2000) Chlorophyll fluorescence—a practical guide. *J Exp Bot* 51(345):659–668
- Nemec P, Nemec I, Nahalkova P, Nemcova Y, Trojanek F, Maly P (2002) Ammonia-free method for preparation of CdS nanocrystalline films by chemical bath deposition technique. *Thin Solid Films* 403:9–12
- O’Sullivan T, Munro EA, Parashurama N, Conca C, Gambhir SS, Harris JS, Levi O (2010) Implantable semiconductor biosensor for continuous in vivo sensing of far-red fluorescent molecules. *Opt Express* 18(12):12513–12525
- Pal R, Yang M, Johnson BN, Burke DT, Burns MA (2004) Phase change microvalve for integrated devices. *Anal Chem* 76(13):3740–3748
- Papageorgiou G (2004) Chlorophyll a fluorescence: a signature of photosynthesis, vol 19. In: *Advances in photosynthesis and respiration*, Springer, Dordrecht
- Suggett D, Oxborough K, Baker N, MacIntyre H, Kana T, Geider R (2003) Fast repetition rate and pulse amplitude modulation chlorophyll a fluorescence measurements for assessment of photosynthetic electron transport in marine phytoplankton. *Eur J Phycol* 38(4):371–384
- Thrush E, Levi O, Cook L, Deich J, Kurtz A, Smith S, Moerner W, Harris J (2005) Monolithically integrated semiconductor fluorescence sensor for microfluidic applications. *Sensor Actuat B Chem* 105(2):393–399. doi:10.1016/j.snb.2004.06.028
- Turner Designs Inc. Turner Designs <http://www.turnerdesigns.com/t2/instruments/cyclops7.html>. Accessed 4 Sept 2010
- Unger MA, Chou H, Thorsen T, Scherer A, Quake SR (2000) Monolithic microfabricated valves and pumps by multilayer soft lithography. *Science* 288(133):113–116
- Yang B, Lin Q (2007) A latchable microvalve using phase change paraffin wax. *Sensor Actuat A Phys* 134:194–200
- Yao B, Luo G, Wang L, Gao Y, Lei G, Ren K, Chen L, Wang Y, Hu Y, Qiu Y (2005) A microfluidic device using a green organic light emitting diode as an integrated excitation source. *Lab on a Chip* 5(10):1041–1047. doi:10.1039/b504959h
- Zimmermann M, Schmid H, Hunziker P, Delamarche E (2007) Capillary pumps for autonomous capillary systems. *Lab on a Chip* 7(1):119–125